

Wide-angle, nonmechanical beam steering using thin liquid crystal polarization gratings

Jihwan Kim,^a Chulwoo Oh,^a Michael J. Escuti,^a Lance Hosting,^b and Steve Serati^b
^aNorth Carolina State Univ, Dept Electrical & Computer Engineering, Raleigh, NC (USA);
^bBoulder Nonlinear Systems Inc, Lafayette, CO (USA)

ABSTRACT

We introduce and demonstrate a compact, nonmechanical beam steering device based on liquid Crystal (LC) Polarization Gratings (PGs). Directional control of collimated light is essential for free-space optical communications, remote sensing, and related technologies. However, current beam steering methods often require moving parts, or are limited to small angle operation, offer low optical throughput, and are constrained by size and weight. We employ multiple layers of LCPGs to achieve wide-angle ($> \pm 40^\circ$), coarse beam steering of 1550 nm light in a remarkably thin package. LCPGs can be made in switchable or polymer materials, and possess a continuous periodic birefringence profile, that renders several compelling properties (experimentally realized): $\sim 100\%$ experimental diffraction efficiency into a single order, high polarization sensitivity, and very low scattering. Light may be controlled within and between the zero- and first-diffraction orders by the handedness of the incident light and potentially by voltage applied to the PG itself. We implement a coarse steering device with several LCPGs matched with active halfwave LC variable retarders. Here, we present the preliminary experimental results and discuss the unique capability of this wide-angle steering.

Keywords: Non-mechanical beam steering, laser radar, laser beam steering, lidar, polarization grating, liquid crystals

1. INTRODUCTION

A nonmechanical beam steering approach is essential to many applications where the optical direction of the instrument changes rapidly to random locations or when the system needs to be relatively compact and have good mechanical stability.^{1,2} Laser communication systems, for example, the beam must be directed to a receiver as tracking precisely with a good mechanical stability, and LIDAR (Light Detection And Ranging) systems need to steer beams over a large field of regard with high precision.

Our approach to nonmechanical beam steering involves two stages: a coarse steering technique combined with a fine steering module as shown in Fig. 1. These two modules may be implemented separately or in combination to offer the coverage and accuracy needed for different applications. In this work we develop and demonstrate a

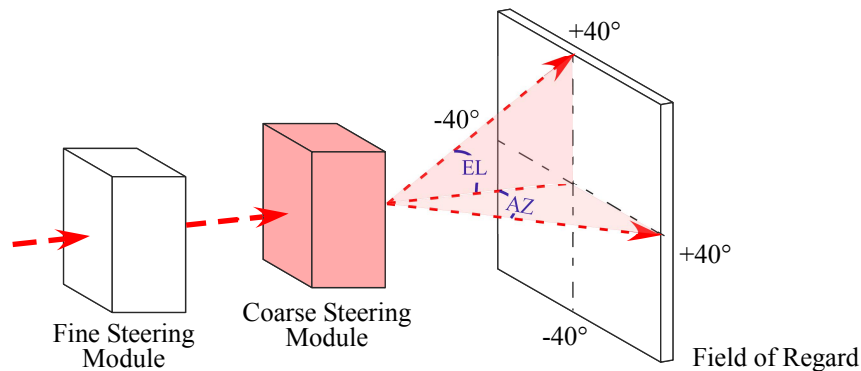


Figure 1. Beam steering system with fine and coarse steering modules providing full 80 x 80 field of regard

Correspondence should be sent to: mjescuti@ncsu.edu, Telephone: +1 919 513 7363

compact two-dimensional coarse steering module based on Liquid Crystal Polarization Gratings³⁻⁵ (LCPGs) that exhibits wide-angle deflection, high overall transmittance, and a very thin package that is practically independent of the steered beam diameter. First we discuss the beam steering properties of LCPGs and then describe a single LCPG stage which will be interlaced for coarse steerer. Then we will look at several possible design options for coarse steering technique and compare their respective efficiencies. Finally, we present experimental data of the proposed coarse steerer.

2. BACKGROUND

2.1 Current Nonmechanical Beam Steering Techniques

A nonmechanical approach for beam steering is desirable since it is likely to be more accurate, faster, compact, lighter, and less expensive than systems using mechanical parts. Such systems find uses in many applications such as optical interconnections,⁶ optical communications,⁷ projection displays,⁸ and so on. Recently several approaches for such nonmechanical beam steering have been developed by different research groups.⁹⁻¹¹

One of the more promising approaches is termed holographic glass,¹² which contains multiple holographic gratings within each glass substrate (usually two or less, in order to minimize scattering and other losses). While efficiency of individual gratings can be quite high, the two inherent limitations of this approach are that (1) two fine-angle steering stages are necessary, and more crucially, that (2) the number of gratings necessary is linearly proportional to the steering angular range. For the sake of discussion, to achieve a range of $\pm 40^\circ$ in one dimension and a resolution of 1.25° , a minimum of 32 glass substrates are required (if each has two multiplexed gratings). This leads to thick systems, and allows the losses of each stage to compound. In comparison to this example, the LCPG approach we introduce here can be configured to reach the same steering range and resolution with as few as 5 gratings.

Another approach uses multiple stages of birefringent prisms¹³ to steer the beam. Each stage adds incremental angular deflections by altering the polarization states at the input of each birefringent prism. But thick prisms are needed for large steering angles, causing significant walkoff, and leading to very long systems where the length is necessarily many times larger than the beam diameter. While our approach is very similar in spirit, we essentially replace the large prisms with a thin diffractive element, thereby dramatically reducing the size, weight, and walkoff. We also expect comparably low losses, near 100% diffraction grating efficiencies, wide-angle operation, and overall thin package potential.

2.2 Liquid Crystal Polarization Grating Basics

The essence of our approach is a nematic LC film with a continuous periodic pattern that can be classified as a Polarization Grating^{3,14,15} (PG). PGs have been studied for many applications, including microdisplays,⁴ tunable filters,¹⁶ spectrophotometers,¹⁷ and imaging spectropolarimeters.¹⁸ Unlike amplitude and phase gratings, PGs operate by modulating the polarization of light. Due to this, PGs can be used for constructing polarization sensitive steering device, capable of highly efficient wide-angle operation.

The structure of LCPG is comprised of an in-plane, uniaxial birefringence that varies with position (i.e $\mathbf{n}(x) = [\sin(\pi x/\Lambda), \cos(\pi x/\Lambda), 0]$), where Λ is the grating period. This structure is created by interfering two orthogonally circular-polarized ultraviolet laser beams recorded within a polarization-sensitive photo-alignment material.^{19,20} This interference leads to the structure illustrated in Fig. 2(a) and (b) where the linear birefringence is embodied in a nematic director $\mathbf{n}(x)$. The ideal diffraction efficiency at normal incidence can be derived with Jones calculus^{14,15,20} as follows:

$$\eta_0 = \cos^2 \left(\frac{\pi \Delta n d}{\lambda} \right), \quad (1)$$

$$\eta_{\pm 1} = \frac{1 \mp S'_3}{2} \sin^2 \left(\frac{\pi \Delta n d}{\lambda} \right). \quad (2)$$

where η_m is the diffraction efficiency of the m diffraction order, Δn is the birefringence of liquid crystal, d is the thickness of the cell, λ is the wavelength of incident light, and $S'_3 = S_3/S_0$ is the normalized Stokes parameter

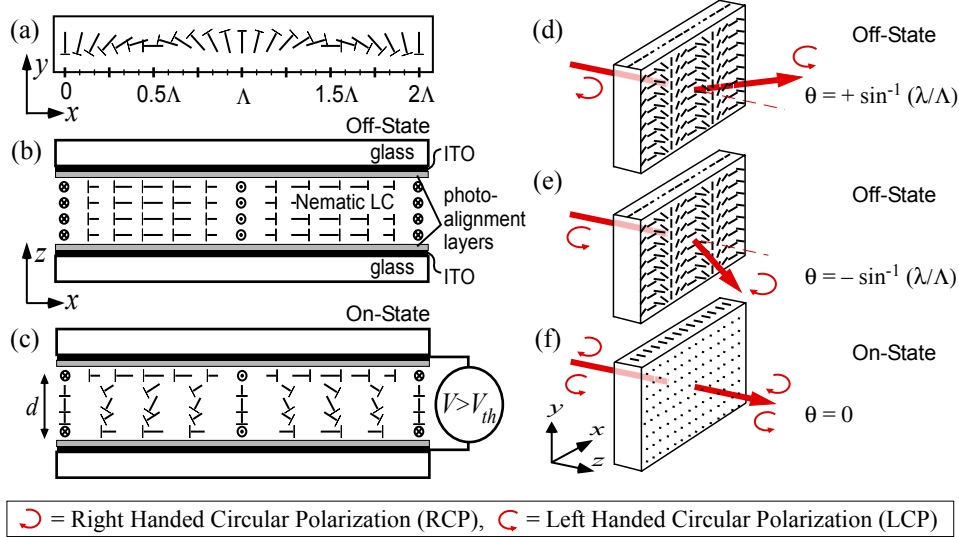


Figure 2. Structure and diffraction properties of the liquid crystal polarization grating (LCPG): (a) Top-view geometry ; (b) Side-view geometry of the continuous, in-plane configuration of the nematic LC with a periodic linear birefringence (Off-state); (c) Side-view geometry with the applied voltage (On-state); Diffraction behavior with (d) RCP and (e) LCP polarized incident light; (f) Incident light transmits on-axis (zero-order diffraction direction) when LCPG is in high voltage state.

corresponding to ellipticity of the incident polarization. Note that the paraxial approximation and a thin grating with the infinite width at normal incidence are assumed to derive the analytical solutions.

From the Eq. 1 and 2, we can derive several properties of LCPG. If the thickness is chosen as $d = \lambda/2\Delta n$ (halfwave retardation of the LC layer), zero-order transmission will be zero ($\eta_0 = 0$) and all of light will deflect to the first orders ($\sum \eta_{\pm 1} = 1$). Moreover, the first orders are highly sensitive with respect to the S'_3 parameter, while the zero-order is polarization independent. Therefore, when the incident light is right handed circular polarization (RCP), $S'_3 = -1$, then diffraction efficiency will be $\eta_{+1} = 1$ and $\eta_{-1} = 0$. This means all of the light passing through the LCPG is diffracted into the positive first order. In the opposite case, if the light is left handed circular polarization (LCP), $S'_3 = +1$, all of the light is defracted into the negative first order ($\eta_{-1} = 1$).

Note that only three diffracted orders are possible (regardless of grating period, thickness, or materials): zero and two first-orders. Moreover, after passing through the LCPG, the handedness of circular polarized light will be changed to the opposite state since the light experiences a relative phase shift due to the LC layer. As shown in Fig. 2(b), once the light of RCP passes through the LCPG, the polarization state would be changed to the LCP. Alternatively, when LCP light goes through the LCPG, passed light would be RCP state (Fig. 2(e)).

The diffraction angles are determined by the well-known grating equation, since the LCPG is merely a birefringent grating.

$$\sin \theta_m = \left(m \frac{\lambda}{\Lambda} \right) + \sin \theta_{in}, \quad (3)$$

where θ_{in} is the incident angle, θ_m is the angle of diffraction of transmitted light, and $m = \{-1, 0, +1\}$ is the diffraction order. The optical communication which uses 1550 nm wavelength light, for instance, needs 8.93 μm grating period of LCPG to perform $\theta = 10^\circ$ diffraction angle. In recent study,³ we found that PGs can retain high diffraction efficiencies for modest incident angles ($\leq 20^\circ$). For the non-diffracting case (zero-order), an applied voltage much greater than a voltage threshold will reorient the LC director out of the plane and reduce the effective birefringence toward zero ($\Delta n \rightarrow 0$) (Fig. 2(c)). By effectively erasing the grating of LCPG, incident light can pass directly through the PG without any change of polarization state. Fig. 3(a) shows the spectral response of the zero-order transmission for different values of applied voltage. If the LCPG is initially designed that no zero order is present in the communication wavelength (1550 nm), an applied voltage which is higher than threshold voltage can erase the gratings and make $\sim 100\%$ zero order transmittance. Fig. 3(b) and

3(c) show polarizing optical microscope images of LCPGs with different applied voltages.²¹ In these images, the LCPG is located between crossed polarizers and the black fringes correspond to areas where the LC molecules are oriented to the one of polarizers' axis. As the voltage is increased, the structure of LCPG loses its periodic nature.

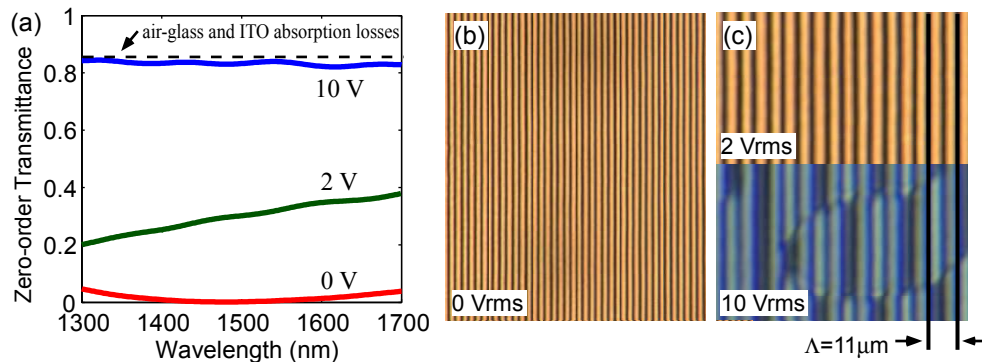


Figure 3. Experimental results: (a) Transmittance spectra of LCPG with applied voltages; (b) Microscope image without applied voltage (0V) and (c) with applied voltage (2V, 10V) higher than threshold

PGs may also be fabricated with polymerizable liquid crystals, known as reactive mesogen²² and enable less scattering losses while allowing for smaller grating periods,²⁰ however, it is impossible to erase the grating with an applied voltage and allow the incident light to pass directly through since gratings of polarimerized PG are fixed indefinitely. We have developed materials and processing methods that offered nearly ideal PGs having > 99.5% experimental diffraction efficiency in the switchable^{4,19,21} and polymer²⁰ type of PGs.

From these properties above, LCPG can efficiently diffract circularly polarized light to either zero or first orders, based on the polarization handedness of the input light and applied voltage. Moreover, PG's thickness is independent of the aperture size and deflection angle, so wide-angle steering with large apertures can be allowed with our device. Since PGs have their own deflection angles inherently according to the grating period, each grating stage can be stacked to double the maximum steered angle in one dimension without major efficiency reductions.

2.3 Fine Angle Steering Module

The fine angle steering module is constructed by using two $1 \times 12,288$ element Optical Phased Arrays (OPAs).²³ We have used two sets of OPAs, implemented at Boulder Nonlinear Systems (BNS), each with a $2\text{cm} \times 2\text{cm}$ aperture as shown in Fig. 4.

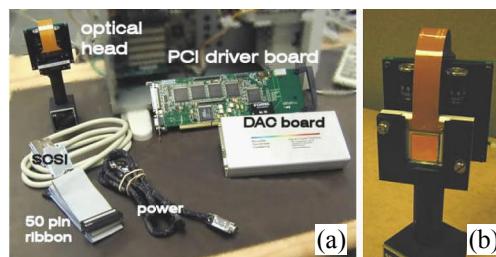


Figure 4. Experimental results: (a) BNS $1 \times 12,288$ OPA coarse beam steering system; (b) Optical head of the system

This 2D fine angle steering system is expected to provide $\sim 90\%$ of throughput: the ratio of output intensity to input intensity. This steering is designed to cover a $\pm 3.125^\circ$ range in both the horizontal and vertical dimensions, and expands the steered beam by a factor of 2.5, thus reducing the steer angle by the same amount. For example, an incident beam with $\pm 3.125^\circ$ coverage and 2cm diameter, will be expanded to a 5cm diameter beam with a $\pm 1.25^\circ$ steering range. Then, this beam passes through the coarse angle steering module having a steering resolution of 1.25° to cover a $\pm 40^\circ$ range in both dimensions.

3. SINGLE LCPG STEERING STAGE

LCPGs can function as highly efficient beam steering elements, by deflecting all of the incident light into one of the three diffraction orders. We have identified several combinations of LCPGs and LC waveplates, that can perform this three-way steering. These designs can be implemented with active or passive PGs, with each approach having its own advantages and disadvantages. In this section we discuss two representative cases, compare the fabrication procedures involved and measure their individual performance.

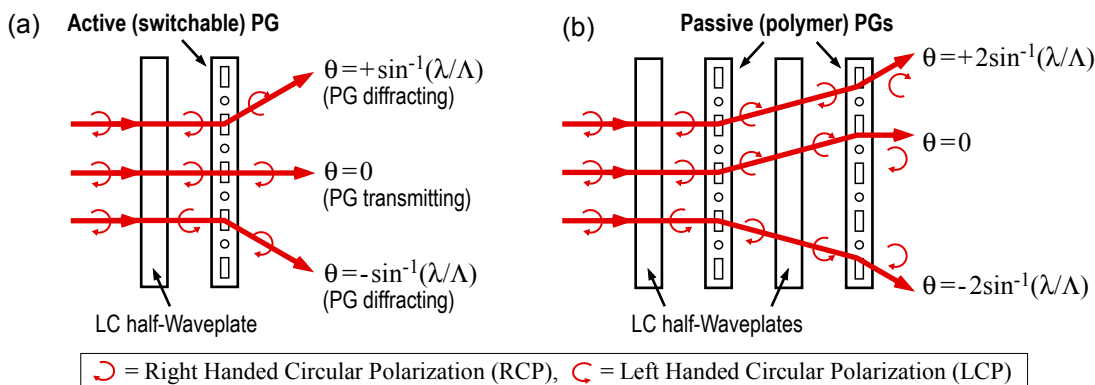


Figure 5. Primary configurations of a single LCPG wide angle stage: (a) "Active PG" stage, with one switchable PG and one variable LC half-waveplate; (b) "Passive PG" stage with two polymer PGs and two variable LC half-waveplates.

Fig. 5(a) describes an active PG beam steering stage, which contains an active PG and an LC half-waveplate. In this scheme, the incident light is assumed to be circularly polarized. The notation for Right Circularly Polarized (RCP) and Left Circularly Polarized (LCP) beams are shown the Fig. 5. Ideally when no voltage is applied, the LC waveplate switches the handedness of the incident light (i.e. RCP \rightarrow LCP or LCP \rightarrow RCP), but under external applied voltage it allows the incoming light to pass through without changing its polarization state. From Eq. 1 and 2, when $d = \lambda/(2\Delta n)$, LCPGs diffract RCP and LCP beams into the +1 and -1 orders respectively, with $\sim 100\%$ efficiency. Hence the polarization sensitive diffraction of LCPGs can be used to select the steering direction into one of the first orders, by simply switching the LC half-waveplate. Moreover, active LCPGs can steer all of the incident light into the zero-order under an applied voltage. Therefore, this active LCPG steering stage can provide three unique steering directions corresponding to the three diffraction orders, by simply switching the voltage across both the elements. Since this approach involves two switchable LC devices, it requires 4 glass substrates and 4 transparent-conducting-electrodes.

In Fig. 5(b), a passive PG steering stage is also able to steer the incident light to three different directions. The stage includes two passive PGs and two variable LC half-waveplates to essentially perform in the same manner as the active PG steering stage. The number of active elements is still the same as before, but this stage uses the two passive PGs, relying on two active LC waveplates for switching the polarization state. Therefore in this stage, the steering directions are determined by the voltage-states of the two LC waveplates, positioned in front of the two passive PGs. When both the waveplates are in same state (i.e. both ON or both OFF), the diffraction from the first PG is compensated by the second one. But when waveplates are in the opposite states, the incident beam can be diffracted into the positive or negative order as shown in Fig. 5 (i.e. RCP \rightarrow + order, RCP \rightarrow - order). So even in this case, three steering directions are possible, and moreover, the passive PGs are firm and thin (polymerized low-molecular weight LC molecules²²) and able to make small grating period, which makes bigger deflection angle. Since this approach involves two switchable LC devices plus two polymer films likely on additional substrates, it requires 6 glass substrates and 4 transparent-conducting-electrodes. Therefore, while the passive PG approach may enable larger angles to be reached, each stage is necessarily thicker and has more interfaces.

4. COARSE STEERER DESIGN OPTIONS

Both the passive and active PG stages discussed in the previous section can steer the incident light into three different directions, according to the voltages applied on their active elements. Several units like these can also be stacked or cascaded to implement a coarse, wide-angle beam steering system with an increased operation range, by arranging each single individual unit appropriately. Such a coarse beam steerer can be engineered to provide wide-angle coverage of $80^\circ \times 80^\circ$ with a resolution of about $1.25^\circ \times 1.25^\circ$.

4.1 Simple Coarse Steerer Design (Binary Switching Within Each Stage)

The coarse beam steerer design in Fig. 6 is based on the binary system, and follows a geometric progression. The diffraction angle of the first stage determines the resolution of coarse beam steerer, and the following stage's diffraction angle is double of previous stage's diffraction angle (e.g. 1.25° , 2.5° , 5° , etc). For a coarse beam steerer consisting of N single stages, a total of 2^{N+1} distinct steering angles are theoretically possible. Therefore, in order to provide $\pm 40^\circ$ coverage with 1.25° resolution, five single stages (i.e. when $N=5$, $2^{N+1}=64$, which also equals the required resolution $2 \times (40^\circ/1.25^\circ)=64$) are needed. As shown in Fig. 6, these single stages (1.25° , 2.5° , 5° , 10° and 20°) are cascaded in different directions to provide two-dimensional steering (AZ, EL). For example, in order to steer the incident light into 22.5° in azimuthal and -16.25° in elevation angles respectively, each stage selectively generates the following states to steer the incident beam in this direction: $2.5^\circ_{(stage2)} + 20^\circ_{(stage5)} = 22.5^\circ$ in AZ and $-1.25^\circ_{(stage1)} - 5^\circ_{(stage3)} - 10^\circ_{(stage4)} = -16.25^\circ$ in EL.

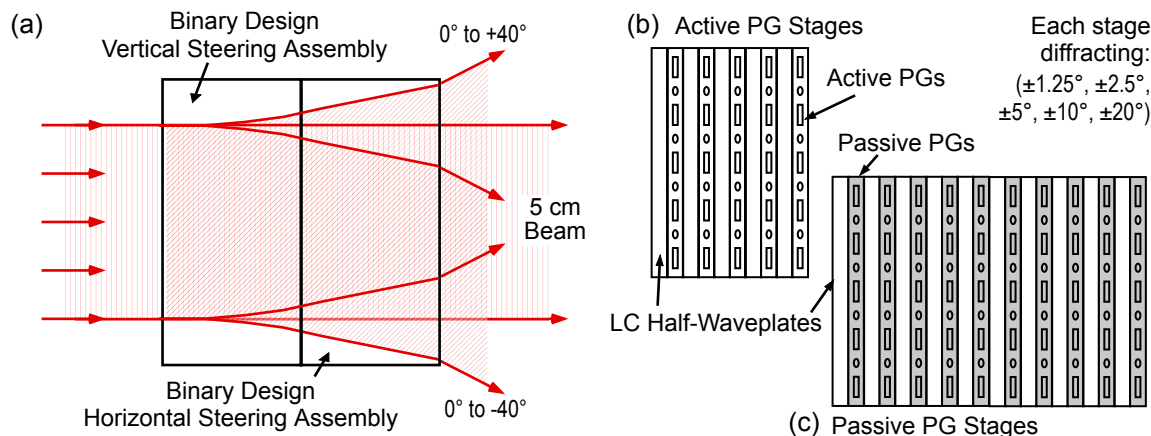


Figure 6. Binary coarse steerer design: (a) Overall construction with 10 single stages (5 for AZ, 5 for EL); each stage can be implemented with (b) Active PGs, or a (c) Passive PGs.

In both this design (Fig. 6) and the design in Section 4.2, the geometric progression is critical. It means that in order to double the field-of-regard in any one dimension, only one additional steering stage or element is necessary. Contrarily, in the holographic glass approach,¹² a doubling of the field-of-regard requires a doubling of the number of stages.

4.2 Improved Coarse Steerer Design (Ternary Switching Within Each Stage)

This coarse beam steerer design (Fig. 7) is based on a ternary (three-state) system, and also follows a geometric progression. The number of elements in coarse steerer needs to be optimized to make the system compact and to reduce losses from these individual units such as absorption from glass, transparent-conducting-electrodes, fresnel reflection losses at different interfaces and scattering from the gratings. While the binary coarse steerer design is fairly simple to understand, it is not the optimal design since it has more than the minimum number of elements. Now we describe another design (based on ternary switching within each stage), which is able to reduce the number of substrates and transparent-conductive-electrodes (see Table 2).

The binary design used an essentially additive approach; it accumulates diffraction angles of each stage as the sign of the directions of angles are all same. However, there could be another way which adds or subtracts

each diffraction angle selectively to make a final steering angle. This is possible because the PGs can make three-way diffraction angles depending on the handedness of incident polarization. This design uses positive and negative direction angles from each PG and the angles may be accumulated selectively according to the applied voltage on PGs. As we discussed in previous section, the handedness of circular polarization would be changed to opposite state when the beam is passing through the PG having halfwave retardation. If the output beam is passing through another PG, the direction of diffraction angle would be opposite from direction of diffraction angle from the previous PG. In this way, when circularly polarized light passes through the multiple PGs, the directions of diffraction angle are to be positive and negative repeatedly. Then, as controlling the applied voltage on each PG, we can accumulate positive or negative diffraction angle by turns.

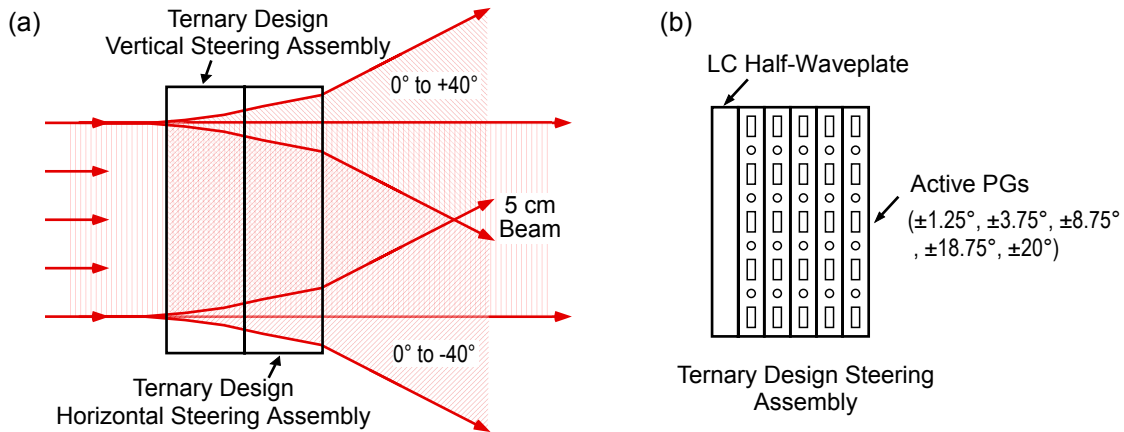


Figure 7. Ternary coarse steerer design: (a) Discrete coarse beam steering accomplished with 10 stages (i.e. 5 in AZ, 5 in EL), but much thinner than Fig. 6(a). However, each stage in this design is a (b) single active PG (without the variable LC half-waveplate). Note that a single variable LC half-waveplate for each dimension (AZ/EL) is still necessary.

Fig. 7(a) shows the improved discrete coarse steerer design implemented with two modified stages. The modified stage consists of one LC half-waveplate and five active PGs having 1.25°, 3.75°, 8.75°, 18.75° and 20° diffraction angles (Fig. 7(b)). The front LC waveplate may change the handedness of incident polarization, and following PGs control the diffraction orders to the zero- or first-order according to the voltages applied them. That means, PGs may pass the beam without changing the angle of beam, or it may deflect the beam to one of the first orders depending on the handedness of incident polarization. Note that the last active PG is interlaced as an antiparalle arrangement comparing with the other PGs, so that the last PG has its anisotropic profile of $\mathbf{n}(x)=[\sin(\pi x/\Lambda), -\cos(\pi x/\Lambda), 0]$, where \mathbf{n} is a unity vector describing the orientation of the linear birefringence. Therefore after passing through the last PG, RCP light is diffracted to negative direction and LCP light diffracted to positive direction in contrast to other PGs. With these configuration of elements, as

Table 1. Applied voltages on each element for ternary discrete coarse steerer design. Note that only a subset (0° to +15°) of the ±40° range is shown.

Elements	State of Applied Voltages												
LCWP	■	■	□	■	□	■	□	■	□	■	□	■	□
PG1 (1.25°)	■	+1.25°	-1.25°	■	■	+1.25°	-1.25°	■	■	+1.25°	-1.25°	■	■
PG2 (3.75°)	■	■	+3.75°	+3.75°	-3.75°	-3.75°	■	■	■	■	+3.75°	+3.75°	-3.75°
PG3 (8.75°)	■	■	■	■	+8.75°	+8.75°	+8.75°	+8.75°	-8.75°	-8.75°	-8.75°	-8.75°	■
PG4 (18.75°)	■	■	■	■	■	■	■	■	+18.75°	+18.75°	+18.75°	+18.75°	+18.75°
PG5 (20.00°)	■	■	■	■	■	■	■	■	■	■	■	■	■
Steering Angle	0°	1.25°	2.5°	3.75°	5°	6.25°	7.5°	8.75°	10°	11.25°	12.5°	13.75°	15°

■ Non-Diffracting State (Voltage ON) □ Diffracting State (Voltage OFF)

shown in Table 1 the improved coarse beam steerer can steer the light with all possible diffraction angles which

can cover proposed field of regard. Table 1 shows the state (ON/OFF) of applied voltage on each element and describes the final steering angles from the modified coarse steerer. Full table is too long so only part of table is presented. This design can work the same as binary design, while this design has less elements. Then, we can expect the increased throughput as well as reduced system losses because fewer elements are used.

4.3 Theoretical Comparison

Having different beam steer designs, we need to estimate the performance between these designs. In order to compare them, we first need to define expected efficiency and losses from each element. There are four main parameters, and for the sake of discussion, we list the nominal best-case-value of each (based in part on our experimental work below):

1. Intrinsic Efficiency - fraction of received light steered into the intended order: >99.5%.
2. Fresnel Loss - loss from reflections at interfaces of differing refractive indices: <0.1%.
3. Absorption Loss - loss due to absorption within the transparent-conducting-electrode layers: <0.2%.
4. Scattering Loss - loss from light randomly scattered by the PGs away from the steered direction: <0.3%.

Table 2. Performance comparison for different coarse steerer designs.

Parameter	Individual value	Binary Passive PG Design		Binary Active PG Design		Ternary Active PG Design	
		Component	Transmittance	Component	Transmittance	Component	Transmittance
Intrinsic Efficiency	99.5%	20	90.5%	10	95.1%	10	95.1%
Fresnel Loss	0.1%	40	96.1%	20	98.0%	12	98.8%
Absorption Loss	0.2%	40	92.3%	40	92.3%	24	95.3%
Scattering Loss	0.3%	20	94.2%	10	97.0%	10	97.0%
Total Transmittance (T)			75.6%		83.4%		86.9%

In Table 2, expected efficiency and losses are shown for different coarse steerer designs. With those parameters, we can expect the total transmittance of each coarse steerer.

$$T = (\eta_{int})^A \cdot (1 - \ell_{fres})^B \cdot (1 - \ell_{abs})^C \cdot (1 - \ell_{scatter})^A \quad (4)$$

where T =total transmittance, η_{int} =intrinsic efficiency, ℓ_{fres} =fresnel loss, ℓ_{abs} =absorption loss, $\ell_{scatter}$ =scattering loss, A =number of PGs, B =number of plates, and C =number of transparent-conducting-electrodes.

From a loss analysis standpoint, the design with the fewest number of elements and transparent-conducting-electrode layers would be the best option. The $80^\circ \times 80^\circ$ improved discrete beam steerer with 1.25° resolution will operate with a total transmittance approximately 87%. Then, as combining with a fine angle steerer whose transmittance is around $\sim 90\%$, the overall transmittance is expected to $\sim 78\%$.

5. EXPERIMENTAL RESULTS

Fig. 8 shows an experimental setup for coarse beam steerer. The polarization state of light coming from a diode laser source (1550 nm) is changed from linear polarized state to circularly polarized state after passing through the quarter-wave plate whose axis at 45° . The circularly polarized light may be deflected to either the zero- or first-order according to the state of applied voltage on PG. To select the direction of the first orders, a half-waveplate can be used for changing the handedness of circular polarization. An IR detector measures the far-field intensity at each diffraction order to calculate the efficiencies and transmittance of PGs.

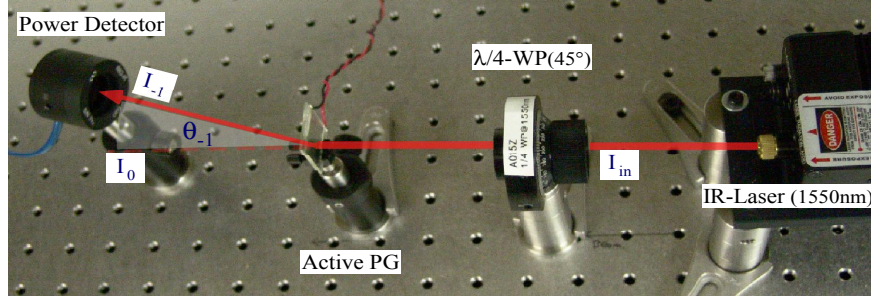


Figure 8. Photograph of the experimental setup to measure the power of diffraction orders. Note that the input beam from the laser is linearly polarized light, and after passing through quarter-wave plate, the beam is changed to circularly polarized light (RCP or LCP). With an applied voltage on active-PG (black&red wires), the beam can be diffracted to zero- or first-order selectively.

5.1 Single PG

We utilized the reactive mesogen mixture RMS03-001C (Merck, $\Delta n = 0.14$ at 1550 nm) for passive PGs, and nematic LC MDA-06-177 (Merck, $\Delta n = 0.13$ at 1550 nm) for active PGs. The thickness of the gratings is $\sim 6.1 \mu\text{m}$ for the halfwave effective PG retardation, $\Delta n d = \lambda/2$. As we discussed diffraction efficiencies with Eq. 1 and 2, if the incident light were circularly polarized, ($S'_3 = \pm 1$), the light would be either diffracted to the first orders depending on the handedness of circular polarization. We used right handed circular polarization (RCP) light as a input, and measured three possible diffraction orders with passive and active PGs having 5° and 10° diffraction angles.

Table 3. Characterization data of single PGs: passive and active types for different diffraction angles ($\lambda = 1550 \text{ nm}$).

Type of PG	$\theta_{\pm 1}$ (deg)	I_{in} (mW)	I_{ref} (mW)	I_{-1} (mW)	I_0 (mW)	I_{+1} (mW)	T_{-1} (%)	η_{-1}^a (%)	η_{-1}^i (%)
passive	± 5	41.32	37.91	37.83	0.07	0.01	91.4	99.6	99.8
passive	± 10	41.32	37.91	37.44	0.07	0.01	91.1	99.3	99.8
active	± 5	41.71	35.68	35.63	0.08	0.01	85.3	99.7	99.8
active	± 10	41.82	35.68	33.71	0.11	0.005	80.6	94.5	99.7

where I_{in} is the input power, I_m is the diffracted power of order m , $T_m = I_m/I_{in}$ is the transmittance of order m , I_{ref} is the transmitted power of substrate/cell filled with glue (used for reference), $\eta_m^a = I_m/I_{ref}$ is the absolute diffraction efficiency of the grating, and $\eta_m^i = I_m/(I_{-1} + I_0 + I_{+1})$ is the intrinsic diffraction efficiency.

Intrinsic efficiency quantifies the inherent diffraction efficiency of the grating alone, normalizing out the effects of the substrates and any scattering. From this data, it is apparent that the efficiency of individual gratings is very high ($> 99.7\%$ for all cases). Absolute diffraction efficiency includes the effect of scattering, but still normalizes out the effect of the substrates. Both polymer and switchable PGs perform with high efficiency ($> 99.3\%$), including scattering. However, the transmittance (including all losses) in these measurements was between 80-91%. It is important to note that almost all of the losses, therefore, were due to the substrates and interfaces (we did not use anti-reflection coatings, nor index-matched ITO). We expect that as we improve the reflection and absorption losses in the substrates by acquiring more optimum glass (AR-coated and index-matched), we will be able to dramatically improve the overall transmittance (toward the optimum values of Sec. 4.3).

Most of losses are primarily in the interface of elements. The reference intensity can be measured with the same element which has no grating. The measured value was almost lower than 90% of the input beam due to the Fresnel and absorption losses driving from the unmatched indices and the transparent-conducting-electrode layers of the surface. The expected throughput will be obtained with the optimized substrates which can reduce the losses with anti-reflection coating and index-matched transparent-conducting-electrode layers.

5.2 Single Stage

Before cascading the PGs and LC half-waveplates, we need to characterize parameters of single stage. First, we measured three different steering directions with 1550 nm wavelength laser for different PG samples having $\pm 5^\circ$

and $\pm 10^\circ$ diffraction angles. Photographs of each diffraction order are achieved with IR sensitive detecting card which is 30 cm off from the PG. Fig. 9(a) shows the detected three orders of the PGs and the different diffraction angles indicated with intervals between the orders; the longer grating period makes the smaller diffraction angle. In Fig. 9(b), the aggregate transmittances (throughputs) are shown for different input properties. Three different conditions make three diffraction orders. Note that the used substrates are not optimized, so aggregate transmittance is lower than what we expect. However, diffraction efficiency is very good; all diffracted beams can be detected at the proposed orders.

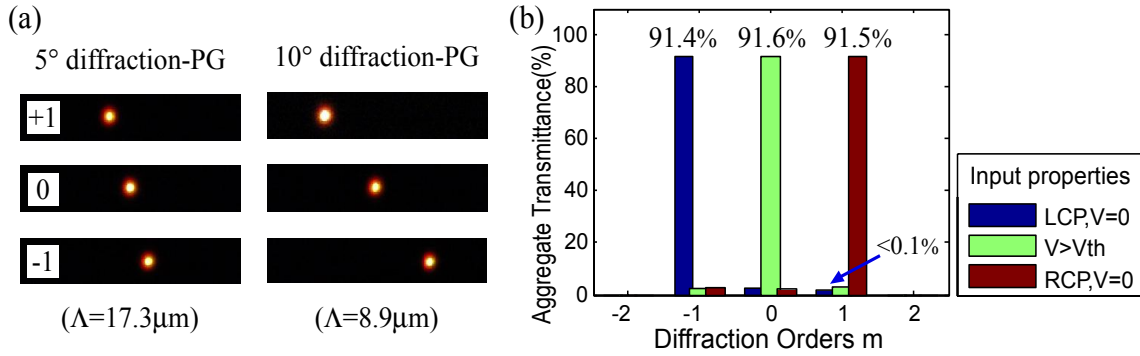


Figure 9. (a) Different diffraction angles, (b) Aggregate Transmittance

5.3 Multi-Stage

We stacked the two single active PG stages to demonstrate seven different steering angles. Using the PGs having $\pm 5^\circ$ and $\pm 10^\circ$ diffraction angles, the stage can selectively control seven steering angles from -15° to $+15^\circ$ with 5° steps. Fig. 10(a) shows the concept of multi-stage achieving more than three steering angles. The multi-stage contains two active PGs and two variable LC half-waveplates, each active element is electrically controlled (switched) with a voltage through the wires.

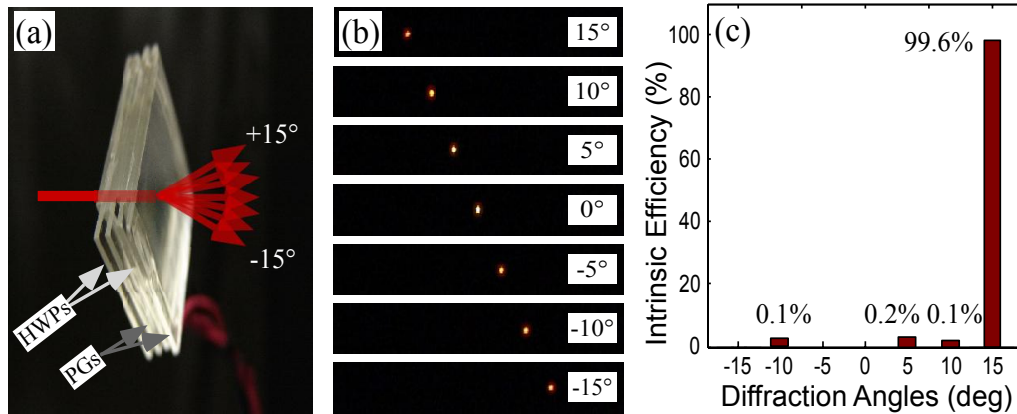


Figure 10. (a) photograph of multi-stage steerer with two active-PGs and two HWPs(half-wave plates); (b) diffracted beams from the multi-stage steerer; (c) intrinsic efficiency of 15-degree diffracted beam

Fig. 10(b) presents seven diffracted beams from the multi-stage steerer. Spots are photographed with an IR sensitive detecting card located 40 cm off from the stage. All diffraction spots are well aligned each other and no significant walkoff was observed. Experimentally demonstrated intrinsic efficiency (steering efficiency) ranges from 99.4% to 99.6% for all seven diffraction beams (with the case of 15° diffraction angle shown in Fig. 10(c)).

6. CONCLUSIONS

Wide-angle nonmechanical beam steerer utilizing polarization gratings (PGs) has been proposed and demonstrated. We have employed multiple layers of PGs for coarse steering, with an ultimate goal of $\pm 40^\circ$ field-of-regard (in both elevation and azimuth) and 1.25° resolution. We show that both passive and active PGs can be used for this coarse beam steerer, with $\sim 100\%$ experimental diffraction efficiency into a single order at 1550 nm. Overall system losses are primarily dependent on the interface and absorption properties of the substrates, and we project that this PG coarse steerer may have overall system transmittance of as high as 87% (with optimum substrates). Finally, note that the coarse steerer thickness is comparably thin, and practically independent of the beam diameter.

ACKNOWLEDGMENTS

The authors gratefully acknowledge support from the US Air Force Research Laboratory (Sensors Directorate), and productive discussions with Dr. Paul McManamon.

REFERENCES

1. P. F. McManamon, T. A. Dorschner, D. I. Corkum, L. J. Friedman, D. S. Hobbs, M. Holz, S. Liberman, H. Q. Nguyen, D. P. Resler, R. C. Sharp, and E. A. Watson, "Optical phased array technology," *Proc. IEEE* **84**(2), pp. 268–298, 1996.
2. P. F. McManamon and E. A. Watson, "Nonmechanical beam steering for passive sensors," *Proc. SPIE* **4369**(1), pp. 140–148, 2001.
3. C. Oh and M. J. Escuti, "Numerical analysis of polarization gratings using the finite-difference time-domain method," *Physical Review A* **76**(4), p. 043815, 2007.
4. R. K. Komanduri, W. M. Jones, C. Oh, and M. J. Escuti, "Polarization-independent modulation for projection displays using small-period lc polarization gratings," *Journal of the Society for Information Display* **15**(8), pp. 589–594, 2007.
5. G. P. Crawford, J. N. Eakin, M. D. Radcliffe, A. Callan-Jones, and R. A. Pelcovits, "Liquid-crystal diffraction gratings using polarization holography alignment techniques," *Journal of Applied Physics* **98**(12), p. 123102, 2005.
6. K. Hirabayashi, T. Yamamoto, and M. Yamaguchi, "Free-space optical interconnections with liquid-crystal microprism arrays," *Appl. Opt.* **34**(14), pp. 2571–2580, 1995.
7. K. Hirabayashi and T. Kurokawa, "Liquid crystal devices for optical communication and information-processing systems," *Liquid Crystals* **14**(2), pp. 307–317, 1993.
8. D. Faklis and G. M. Morris, "Diffractive optics technology for display applications," *Proc. SPIE* **2407**(1), pp. 57–61, 1995.
9. X. Wang, B. Wang, P. J. Bos, J. E. Anderson, J. J. Pouch, F. A. Miranda, and P. F. McManamon, "Wide angle liquid crystal optical phased array," *OSA Technical Digest*, 2004.
10. H. H. Refai, J. J. Sluss, and M. P. Tull, "Digital micromirror device for optical scanning applications," *Optical Engineering* **46**(8), 2007.
11. M. T. Johnson and G. S. Seetharaman, "Thermo-optic variable blazed grating for beam steering," *Proc. SPIE* **6715**(1), p. 671505, 2007.
12. L. B. Glebov, "Photosensitive holographic glass - new approach to creation of high power lasers," *European Journal of Glass Science and Technology* **48**(3), pp. 123–128, 2007.
13. J. Shi, P. J. Bos, B. Winker, and P. F. McManamon, "Switchable optical phased prism arrays for beam steering," *Proc. SPIE* **5553**(1), pp. 102–111, 2004.
14. L. Nikolova and T. Todorov, "Diffraction efficiency and selectivity of polarization holographic recording," *Optica Acta* **31**(5), pp. 579–588, 1984.
15. J. Tervo and J. Turunen, "Paraxial-domain diffractive elements with 100% efficiency based on polarization gratings," *Optics Letters* **25**(11), pp. 785–786, 2000.

16. E. Nicolescu and M. J. Escuti, "Polarization-independent tunable optical filters based on liquid crystal polarization gratings," *Proc. SPIE* **6654**(1), 2007.
17. E. Nicolescu and M. J. Escuti, "Compact spectrophotometer using polarization-independent liquid crystal tunable optical filters," *Proc. SPIE* **6661**(1), 2007.
18. J. Kim and M. J. Escuti, "Snapshot imaging spectropolarimeter utilizing polarization gratings," *Proc. SPIE* **7086**, 2008.
19. M. J. Escuti and W. M. Jones, "A polarization-independent liquid crystal spatial light modulator," *Proc. SPIE* **6332**(1), 2006.
20. M. J. Escuti, C. Oh, C. Sanchez, C. Bastiaansen, and D. J. Broer, "Simplified spectropolarimetry using reactive mesogen polarization gratings," *Proc. SPIE* **6302**(1), 2006.
21. M. J. Escuti and W. M. Jones, "Polarization-independent switching with high contrast from a liquid crystal polarization grating," *SID Int. Symp. Digest* **37**(2), pp. 1443–1446, 2006.
22. S. M. Kelly, "Anisotropic networks," *J. Mater. Chem.* **5**(12), pp. 2047–2061, 1995.
23. A. Linnenberger, S. Serati, and J. Stockley, "Advances in optical phased array technology," *Proc. SPIE* **6304**(1), 2006.